

## NUMERICAL ANALYSIS OF DUCTILE FRACTURE

Jelena ŽIVKOVIĆ<sup>1</sup>, Vladimir DUNIĆ<sup>1</sup>, Miroslav ŽIVKOVIĆ<sup>1</sup>, Nenad GRUJOVIĆ<sup>1</sup>

<sup>1</sup> University of Kragujevac, Faculty of Engineering, Sestre Janjić 6, 34000 Kragujevac, Serbia,  
E-mail: [jelena.zivkovic@kg.ac.rs](mailto:jelena.zivkovic@kg.ac.rs); [dunic@kg.ac.rs](mailto:dunic@kg.ac.rs); [miroslav.zivkovic@kg.ac.rs](mailto:miroslav.zivkovic@kg.ac.rs); [gruja@kg.ac.rs](mailto:gruja@kg.ac.rs)

### 1. Introduction

The largest issue in fracture mechanics is the lack of possibility to detect damage nucleation and the way it will merge into a new initial crack. This paper presents a comparison of numerical results given in [1], obtained by using the phase-field model for ductile fracture of elasto-plastic solids, and numerical results obtained by using in-house software package PAK [2], for calculations of structures based on the Finite Element Method. The numerical analysis was done for the example of tension of Steel-1.0553 flat specimen.

### 2. Large strain analysis

The stress integration algorithm of large strain deformations in isotropic plasticity based on the multiplicative decomposition of the deformation gradient, using the logarithmic strains, is given:

1. Determination of the relative and normalized relative deformation gradient

$${}^{t+\Delta t} \mathbf{F} = \mathbf{1} + \frac{\partial^{\Delta t} \mathbf{u}}{\partial^t \mathbf{x}}, \quad {}^{t+\Delta t} \bar{\mathbf{F}} = \left| {}^{t+\Delta t} \mathbf{F} \right|^{-\frac{1}{3}} {}^{t+\Delta t} \mathbf{F}$$

2. Elastic trial solution

$${}^{t+\Delta t} \bar{\mathbf{b}}^{E*} = {}^{t+\Delta t} \bar{\mathbf{F}}^T {}^t \bar{\mathbf{b}}^E {}^{t+\Delta t} \bar{\mathbf{F}} = \sum_{A=1}^3 (\bar{\lambda}_A^{E*})^2 \mathbf{q}_A \otimes \mathbf{q}_A$$

$${}^{t+\Delta t} \bar{\mathbf{e}}^{E*} = \sum_{A=1}^3 \ln(\bar{\lambda}_A^{E*}) \mathbf{q}_A \otimes \mathbf{q}_A$$

3. Determination of the trial deviatoric elastic stress tensor and trial equivalent elastic stress:

$${}^{t+\Delta t} \mathbf{S}^{E*} = G \text{dev} {}^{t+\Delta t} \bar{\mathbf{b}}^{E*}, \quad {}^{t+\Delta t} \sigma^{E*} = \sqrt{\frac{3}{2}} \left\| {}^{t+\Delta t} \mathbf{S}^{E*} \right\|$$

4. Checking of yield condition

$${}^{t+\Delta t} f_y^E = {}^{t+\Delta t} \sigma^{E*} - {}^t \sigma_y \leq 0 \text{ - elastic sol., go to 6}$$

5. Calling the program for the integration of constitutive relations [3, 4] to determine

deviatoric stress tensor and determinant of plastic deformation gradient

$${}^{t+\Delta t} \sigma = \sqrt{\frac{3}{2}} \left\| {}^{t+\Delta t} \mathbf{S} \right\|$$

$$\left| {}^{t+\Delta t} f_y \right| = \left| {}^{t+\Delta t} \sigma - {}^t \sigma_y \right| > 0 \text{ - new iter., go to 5}$$

6. Deformation gradient and determinant of elastic deformation gradient using multiplicative decomposition

$${}^{t+\Delta t} \mathbf{F} = {}^{t+\Delta t} \mathbf{J}^T \left( {}^0 \mathbf{J}^{-1} \right)^T \quad \left| {}^{t+\Delta t} \mathbf{F}_E \right| = \frac{\left| {}^{t+\Delta t} \mathbf{F} \right|}{\left| {}^t \mathbf{F}_P \right|}$$

7. Final stress solution

$$\sigma_m = c_m e_m \quad e_m = \frac{1}{3} \left( \left| {}^{t+\Delta t} \mathbf{F}_E \right| - 1 \right)$$

$$c_m = \frac{E}{1-2\nu} \quad {}^{t+\Delta t} \sigma = {}^{t+\Delta t} \mathbf{S} + \sigma_m \mathbf{1}$$

8. Correction of elastic configuration at the end of the step

$${}^{t+\Delta t} \bar{\mathbf{b}}^E = \frac{1}{G} {}^{t+\Delta t} \mathbf{S} + \bar{\mathbf{b}}_m^E \mathbf{1} \quad \bar{\mathbf{b}}_m^E = \frac{1}{3} {}^{t+\Delta t} \bar{\mathbf{b}}_{ii}^{E*}$$

### 3. Numerical results

In this section we investigate the ability of our in-house software PAK to capture representative aspects of the fracture process in ductile materials. The numerical analysis was done on flat tensile specimen made of Steel 1.0553 shown in Fig.1. The specimen is modeled using the 3D solid elements with 8 and 20 nodes per element. An elastic-plastic material model with isotropic hardening was used. Hardening zone is described by Ramberg-Osgood's

curve  ${}^t \sigma_y = \sigma_{yv} + C_y \left( {}^t \bar{\epsilon}^p \right)^n$ . Material parameters for hardening law proposed by Simo, [5], used in [1] were fitted for Ramberg-Osgood's law, Fig.2.

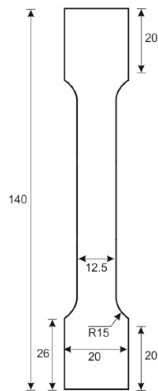


Fig. 1. Flat tensile specimen Steel-1.0553.

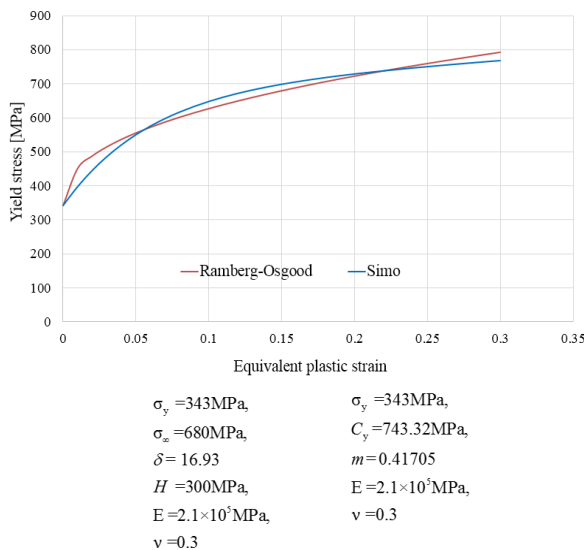


Fig. 2. Simo and Ramberg-Osgood hardening curves.

Fig. 3 shows a comparison of load-displacement curves for the results obtained by software PAK, for solid 8-node and 20-node elements (RO8 and RO20 in Figure 3, respectively), and the results given in [1] for phase-field model, elasto-plastic model without phase-field and the results obtained experimentally.

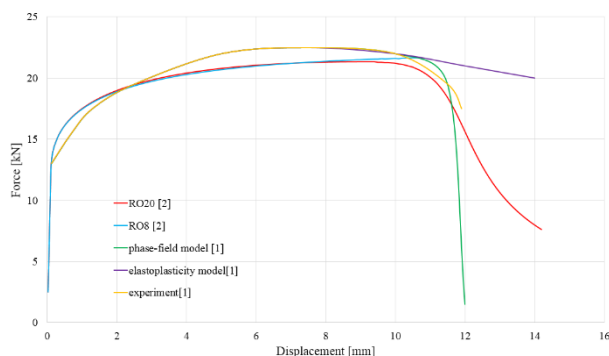


Fig. 3. Load-displacement curves for flat tensile specimen Steel-1.0553.

The results of elastoplastic model with phase-field predicts crack initiation and propagation, but so as the results of elastoplastic model in PAK in case of 20-node elements. During the numerical simulation it was observed that as the deformation progresses, equivalent plastic strain concentrates in the necking zone, taking the maximum value in the middle of the specimen and it is followed by propagation towards the edge of the specimen.

#### 4. Conclusions

This paper shows comparison of results obtained by using the software package PAK with the results given in [1] obtained by experiment, and the elastoplastic model with and without phase-field. The comparison was done in order to investigate the ability of PAK to capture representative aspects of fracture in ductile materials.

It is shown that the elastoplastic model in PAK gives similar results as the model with the phase-field given in [1]. Model used for calculations in this paper showed that it can capture sequence of elastoplastic deformation and necking in flat specimens in case of solid 20-node elements. As the deformation progresses, the equivalent plastic strain concentrates in the necking zone, taking the maximum value in the middle of the specimen and it is followed by propagation towards the edge, which corresponds with experimental observations.

#### Acknowledgements

The part of this research is supported with the Project TR32036 financed by the Ministry of Education, Science and Technological Development, Republic of Serbia

#### References

- [1] Ambati, M., et al., A phase-field model for ductile fracture at finite strains and its experimental verification. *Computational Mechanics*, 2016, 57, pp. 149-167
- [2] Kojić, M., et al., PAK-S: Program for FE Structural Analysis, Faculty of Mechanical Engineering, University of Kragujevac, Kragujevac, Serbia, 1999
- [3] Kojić, M., Bathe, K.J., *Inelastic Analysis of Solids and Structures*, Springer-Verlag Berlin Heidelberg, 2005, ISBN 3-540-22793-8
- [4] Živković, M., *Nelinearna analiza konstrukcija*, Univerzitet u Kragujevcu, Mašinski fakultet, ISBN 86-80581-59-3, Kragujevac, 2006
- [5] Simo, J.C., Hughes, T.J.R., *Computational Inelasticity*, Interdisciplinary applied mathematics, Springer-Verlag Berlin Heidelberg, 2000, ISBN 0-387-97520-9